Refined measurements of piezooptic coefficient π_{66} for the lithium niobate crystals, using a crystalline disk compressed along its diameter

Savaryn V., Krupych O. and Vlokh R.

Institute of Physical Optics, 23 Dragomanov Str., 79005 Lviv, Ukraine,
e-mail: ok@ifo.lviv.ua

Received: 03.02.2014

Abstract. We have checked the accuracy and reliability of an experimental technique suggested earlier for determining piezooptic coefficients. It is based on inducing a predefined 2D distribution of mechanical stresses in a transparent material disk compressed along its diameter. We have shown that the technique enables to measure the piezoopic constants with high enough accuracy. The sources of experimental errors are thoroughly analyzed and eliminated. The experimental procedures are presented in detail for the case of measurements of the parameter $\pi_{66} = \pi_{11} - \pi_{12}$ for the crystalline disk of lithium niobate. Our results conform well to the literature data and evidence high reliability and precision of the technique.

Keywords: piezooptic effect, 2D spatial stress distribution, crystalline disks, lithium niobate

PACS: 78.20.H-, 78.20.Ci, 07.10.Lw
UDC: 535.012

1. Introduction

Nowadays optical materials are used in a wide class of applications like acoustooptic and electrooptic devices, photoelasticity, stress tensor field tomography, remote optical stress sensors, photoelastic modulators of light polarization, etc. Comprehensive and consistent characterization of these materials requires knowledge of photoelastic and piezooptic properties [1–8]. It is known that a piezooptic effect consists in changes of refractive indices of an optical material in response to mechanical stresses. It may be written in terms of a tensor relation initially suggested by F. Pockels [9, 10]:

$$\delta B_\lambda = \delta\left(\frac{1}{n^2}\right)_\lambda = \pi_{\lambda\mu}\sigma_\mu \quad (\lambda, \mu = 1\ldots6), \tag{1}$$

where the Voigt notation is used. In Eq. (1), δB_λ denotes the increment of a specific component of optical impermeability tensor, n_λ the relevant refractive index, σ_μ the stress tensor components, and $\pi_{\lambda\mu}$ the components of a fourth-rank tensor of piezooptic coefficients (POCs).

Usually the POCs $\pi_{\lambda\mu}$ are measured with relatively high errors. The latter are mainly caused by a non-uniform 3D spatial distribution of the stress components generated in real parallelepiped-shaped samples under a uniaxial pressure [11], whereas a spatially uniform stressed state is almost forcedly assumed by the common theoretical models. Recently, a number of measuring techniques have been developed by our scientific group to improve the accuracy of POC determination. They make use of the loading methods which give rise to non-uniform, though known in advance, stress

distributions in a sample. These are a measuring technique based on crystal torsion [12–14], a combination of digital imaging laser interferometry with a classical four-point bending method [15–17], and a technique based on compressing of crystalline disks along their diameters [18].

The last of the above methods has earlier been tested on the example of crystalline disk made of well-known single crystals of lithium niobate ($LiNbO_3$, abbreviated hereafter as LN). LN is an optically uniaxial crystal widely used as a nonlinear optical material. Our study [18] has resulted in the magnitude of the POC $|\pi_{66}| = |\pi_{11} - \pi_{12}|$ obtained experimentally using the imaging polarimetry. In the units of Brewster ($1\text{B} = 10^{-12}$ m^2/N) it is equal to $|\pi_{66}| = 0.20\pm0.01$ B. This parameter is smaller than that reported earlier in the work of Mytsyk et al. [19] ($\pi_{66} = \pi_{11} - \pi_{12} = -0.47$ B) where an interferometric technique and a common loading scheme have been employed. Of course, this evident discrepancy between the POC values may be explained by a higher experimental error reported by the authors of Ref. [19] (~ 15%), as well as some peculiarities of their experimental procedures concerned with accounting for the Poisson strain in a sample and piezoelectric contribution into the optical retardation. However, some time later a full POC matrix for the LN has been measured with the method based on the four-point bending [17]. According to that study performed also by our scientific group, the POC under interest is equal to $\pi_{66} = \pi_{11} - \pi_{12} = -0.573\pm0.079$ B.

Hence, it is evident that the POC π_{66} of the LN measured in the work [18] for a compressed LN disk deviates significantly from the results derived with the other experimental techniques, and the reasons seem to be not so simple. Therefore we have decided to reinvestigate the above POC under the same experimental conditions as in the study [18], in particular the same orientation of the single crystal, the loading scheme and the configuration of our imaging polarimeter.

2. Experimental technique

The experimental technique used here has been described in detail in our previous works (see [18]). Therefore, below we will illustrate only the key points of the method for the convenience of readers. It is known [20] that loading of a thin disk along its diameter forms a 2D stressed state. When the disk is cut perpendicular to the principal axis Z of the crystal and the loading force P is applied along Y axis, the three components of the stress tensor $\hat{\sigma}$ appear. They are spatially distributed in the XY plane in the following manner [20]:

$$\sigma_1 = \sigma_x = -\frac{2P}{\pi d}\left[\frac{(R-Y)X^2}{\left(X^2+(R-Y)^2\right)^2} + \frac{(R+Y)X^2}{\left(X^2+(R+Y)^2\right)^2} - \frac{1}{2R}\right], \tag{2a}$$

$$\sigma_2 = \sigma_y = -\frac{2P}{\pi d}\left[\frac{(R-Y)^3}{\left(X^2+(R-Y)^2\right)^2} + \frac{(R+Y)^3}{\left(X^2+(R+Y)^2\right)^2} - \frac{1}{2R}\right], \tag{2b}$$

$$\sigma_6 = \tau_{xy} = \frac{2P}{\pi d}\left[\frac{(R-Y)^2 X}{\left(X^2+(R-Y)^2\right)^2} - \frac{(R+Y)^2 X}{\left(X^2+(R+Y)^2\right)^2}\right]. \tag{2c}$$

Here d is the thickness of the disk and R its radius. Now consider the particular case of LN. The POC tensor for the point group 3m, to which LN belongs, may be represented as

$$\pi_{qm} = \begin{pmatrix} \pi_{11} & \pi_{12} & \pi_{13} & \pi_{14} & 0 & 0 \\ \pi_{12} & \pi_{11} & \pi_{13} & -\pi_{14} & 0 & 0 \\ \pi_{31} & \pi_{31} & \pi_{33} & 0 & 0 & 0 \\ \pi_{41} & -\pi_{41} & 0 & \pi_{44} & 0 & 0 \\ 0 & 0 & 0 & 0 & \pi_{44} & 2\pi_{41} \\ 0 & 0 & 0 & 0 & \pi_{14} & (\pi_{11}-\pi_{12}) \end{pmatrix}. \tag{3}$$

When the probing light propagates along the Z axis, the optical birefringence appearing inside the compressed disk is determined as [18]

$$\Delta n_{12} = -\frac{1}{2} n_o^3 (\pi_{11}-\pi_{12}) \sqrt{(\sigma_1-\sigma_2)^2 + 4\sigma_6^2}\ , \tag{4}$$

(n_o – is the ordinary refractive index) while the optical retardation Γ accessible for experimental measurements looks as

$$\Gamma = \frac{2\pi d}{\lambda} \Delta n_{12} = -\frac{\pi d}{\lambda} n_o^3 (\pi_{11}-\pi_{12}) \sqrt{(\sigma_1-\sigma_2)^2 + 4\sigma_6^2}\ . \tag{5}$$

Since, according to Eqs. (2), the stress tensor components σ_μ included in Eq. (5) depend on the coordinates X and Y, we arrive at a 2D spatial distribution of the optical retardation Γ. Notice that a spatial map of the Γ parameter can be readily measured by means of our imaging polarimeter. Therefore the analysis of experimental 2D spatial distribution of Γ should give us the magnitude of the POC difference ($\pi_{11} - \pi_{12}$) which is equal to π_{66} in the case of LN (see Eq. (3)).

Examination of Eq. (2c) leads to conclusion that the stress tensor component σ_6 vanishes whenever (i) $X = 0$ or (ii) $Y = 0$. The first condition corresponds to the points located on the disk diameter along which the loading force acts, whereas the second corresponds to the diameter perpendicular to the applied force. Eq. (5) is simplified for those diameters to

$$\Gamma = -\frac{\pi d}{\lambda} n_o^3 \pi_{66} (\sigma_1 - \sigma_2)\,. \tag{6}$$

If we have $\sigma_6 = 0$, the angle ζ_3 of the optical indicatrix rotation around the Z axis is also equal to zero. The latter fact is in accord with the relation [18]

$$\tan 2\zeta_3 = \frac{2\sigma_6}{\sigma_1 - \sigma_2}\,, \tag{7}$$

thus implying that, under compression of the disk, the principal axes of the optical indicatrix should not rotate for the two diameters mentioned above.

Now let us consider an experimental geometry called as a ‘loading’ diameter and defined by the equality $X = 0$. The retardation Γ along this diameter is determined as [18]

$$\Gamma = -\frac{\pi d}{\lambda} n_o^3 \pi_{66} \frac{2RP}{\pi d\left(R^2 - Y^2\right)} = -\frac{2P}{\lambda} n_o^3 \pi_{66} \frac{R}{R^2 - Y^2}\,. \tag{8}$$

Finally, the dependence of the retardation Γ on the X coordinate for a geometry called as a ‘perpendicular’ diameter ($Y = 0$) reads as (see [18])

$$\Gamma = -\frac{\pi d}{\lambda} n_o^3 \pi_{66} \frac{2P}{\pi d} \frac{R(R^2 - X^2)}{(R^2 + X^2)^2} = -\frac{2P}{\lambda} n_o^3 \pi_{66} \frac{R(R^2 - X^2)}{(R^2 + X^2)^2}\,. \tag{9}$$

It is obvious that the POC π_{66} can be easily determined from fitting of experimental dependences

of the retardation Γ on the appropriate coordinates taken along the 'loading' and 'perpendicular' diameters, and the fitting functions are defined respectively by Eq. (8) and Eq. (9).

We have used an imaging polarimeter of which setup is described in Ref. [21]. The polarimeter is built according to a standard PCSA (polarizer–compensator–sample–analyzer) scheme. In the particular configuration used in the present work, we have made the probing beam circularly polarized, thus making the measuring procedure insensitive to orientation of the optical indicatrix inside the sample. In general, the polarization of light passing through the sample becomes elliptic, with the ellipticity defined by the retardation and the azimuth of long axis of ellipse, determined by the orientation of the optical indicatrix. To analyze the polarization state of the light emergent from the sample, the azimuth of the analyzer is scanned and a corresponding set of images is obtained. Then fitting of the azimuthal dependences of the intensity recorded by a CCD camera is performed for each pixel of the sample image. One can thus construct 2D maps of the optical anisotropy parameters of the sample, i.e. the optical retardation (the phase difference) and the optical indicatrix orientation.

3. Experimental results

A sample in the shape of a disk was made from the Z cut of LN, with the diameter of 13.74 mm and the thickness of 2.32 mm (see Fig. 1). The loading force was directed parallel to the Y axis (i.e., vertically).

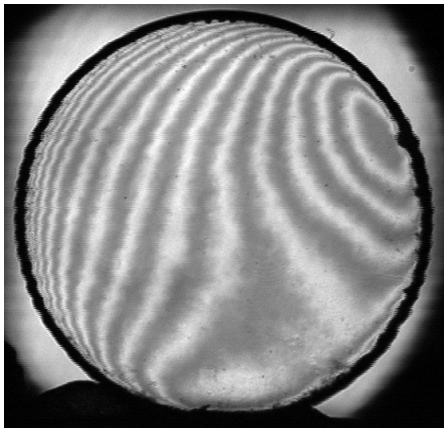

Fig. 1. Appearance of LN sample in the field of view of our polarimeter. Fringes are caused by multiple light reflections from sample faces and indicate to a small deviation from their parallelism.

To provide a circular polarization of the probing beam, initially we aligned the fast axis of the compensator parallel to the transmission axis of the polarizer. This azimuth of the compensator is denoted as C_0. Then the compensator was rotated to the angular orientation $C_1 = C_0 - 45°$.

Maps of the optical retardation and the orientation of indicatrix of the sample were obtained experimentally for the loading forces equal to 0, 16.30 and 57.06 N. Examples of the experimental maps are presented in Fig. 2. In general, they agree well with the theoretical maps calculated from Eqs. (2) and Eq. (5).

The next step was subtracting the retardation maps obtained under the loads of 57.06 N and 16.30 N. The map for this retardation difference $\Delta\Gamma$ is shown in Fig. 3. The coordinate dependences of $\Delta\Gamma$ for the both geometries associated with the 'loading' and 'perpendicular' diameters were taken from this map. The dependence of $\Delta\Gamma$ on the X coordinate for the 'perpendicular' diameter was fitted by the function analogous to that given by Eq. (9), in which P and Γ were substituted by ΔP and $\Delta\Gamma$:

$$\Delta\Gamma = -\frac{2(\Delta P)}{\lambda} n_o^3 \pi_{66} \frac{R(R^2 - X^2)}{(R^2 + X^2)^2}. \tag{10}$$

Fig. 4a depicts both the experimental data and the fitting curve. The fitting has resulted in the POC value $\pi_{66} = -0.571 \pm 0.012$ B.

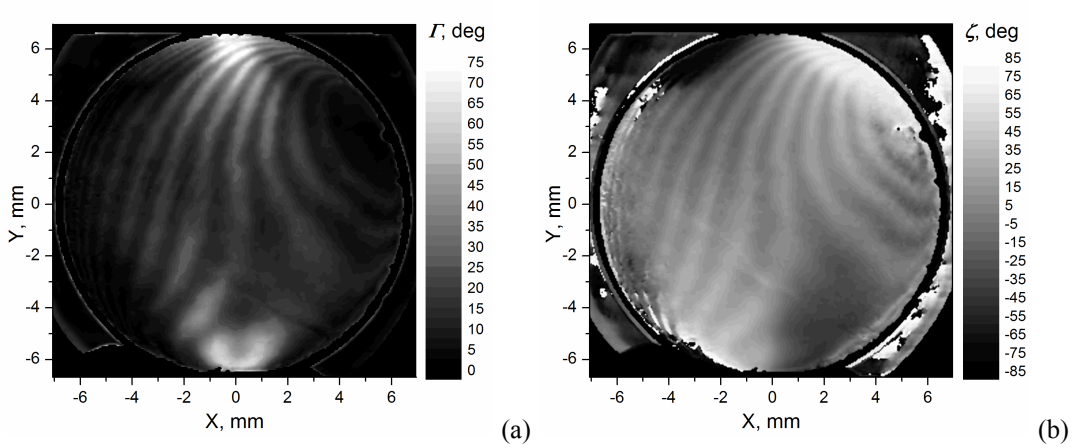

Fig. 2. *XY* maps of retardation (a) and optical indicatrix orientation (b) induced in the LN disk by the loading force 57.06 N (λ = 632.8 nm). Compensator position is given by $C_1 = C_0 - 45°$.

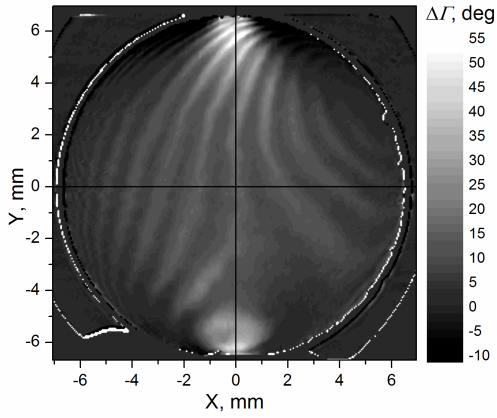

Fig. 3. *XY* map of retardation difference induced in the LN disk under loading force change from 16.30 N to 57.06 N (λ = 632.8 nm). Compensator position is given by $C_1 = C_0 - 45°$.

The dependence $\Delta\Gamma$ on the Y coordinate obtained for the case of 'loading' diameter was fitted by the function analogous to Eq. (8),

$$\Delta\Gamma = -\frac{2(\Delta P)}{\lambda} n_o^3 \pi_{66} \frac{R}{R^2 - Y^2}. \tag{11}$$

It is seen from Eq. (1) that the denominator tends to zero in the vicinity of points where the loading force is applied ($|Y| \to R$), thus leading to singular behaviour of the $\Delta\Gamma$ parameter. This ensues from Eqs. (2), in which the stress component σ_2 becomes infinite when $X = 0$ and $|Y| = R$. Therefore Eqs. (2) represent a restricted model which is not applicable for the regions close to the points where the loading force is applied. Then a natural question arises concerning the limits where Eq. (11) can be correctly applied while fitting the experimental data. We have investigated this problem. As seen from Fig. 4b, the fitting has been performed for the three cases: (1) the full data range (i.e., all of the data collected are used in the fitting procedure), (2) the data from the interval $|Y| < 6$ mm $\approx 0.88R$, and (3) the data from the interval $|Y| < 5.5$ mm $\approx 0.80R$. We have

obtained the following POC values (1) $\pi_{66} = -0.359 \pm 0.011$ B, (2) $\pi_{66} = -0.480 \pm 0.010$ B, and (3) $\pi_{66} = -0.508 \pm 0.010$ B. One can see that narrowing data region used for fitting is followed by approaching the π_{66} value to that obtained with the data of 'perpendicular' diameter. Further decrease of the data region would result in 'saturating' the POC value and, simultaneously, less reliability of the fitting due to negative influence of multiple reflection fringes. Therefore we conclude that the optimal data region for the case of 'loading' diameter is $|Y| < 0.80R$, so that the POC value $\pi_{66} = -0.508 \pm 0.010$ B is most consistent.

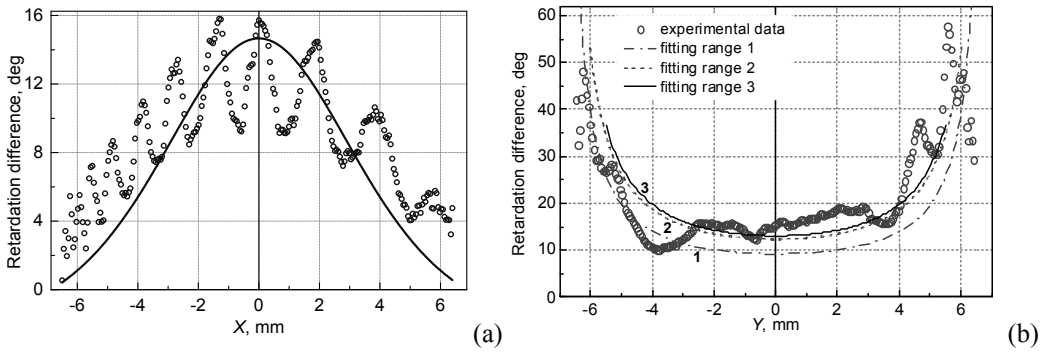

Fig. 4. Dependences of retardation difference $\Delta\Gamma$ on the *X* coordinate along the 'perpendicular' diameter (a) and on the *Y* coordinate for the 'loading' diameter (b) for the LN disk, as measured under loading force change from 16.30 to 57.06 N (λ = 632.8 nm). Compensator position is given by $C_1 = C_0 - 45°$.

To further improve trueness of the measured π_{66} value, we have repeated the procedures described above for the opposite sign of circular polarization of the probing beam. This can be realized by setting the compensator at the azimuth $C_2 = C_0 + 45°$. As a result, we have obtained the POC $\pi_{66} = -0.502 \pm 0.009$ B for the case of 'perpendicular' diameter (see Fig. 5a) and $\pi_{66} = -0.450 \pm 0.008$ B for the case of 'loading' diameter (see Fig. 5b).

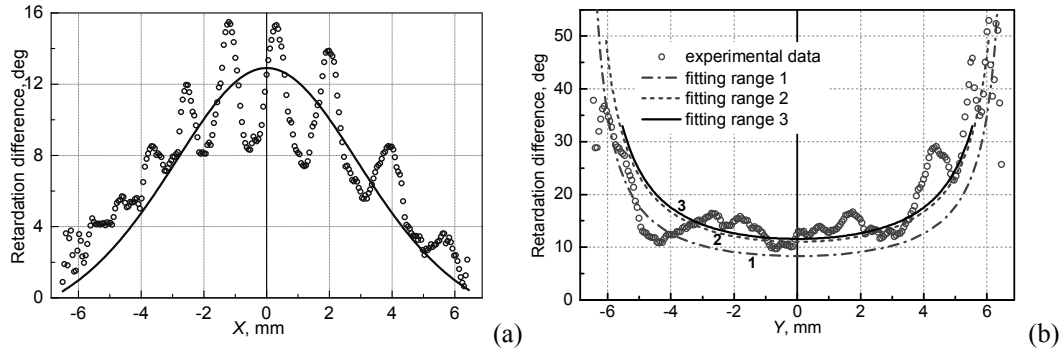

Fig. 5. Dependences of retardation difference $\Delta\Gamma$ on the *X* coordinate along the 'perpendicular' diameter (a) and on the *Y* coordinate for the "loading" diameter (b) for the LN disk, as measured under loading force change from 16.30 N to 57.06 N (λ = 632.8 nm). Compensator position is given by $C_2 = C_0 + 45°$.

We have calculated the mean POC and the corresponding error from the four values given above: $\langle \pi_{66} \rangle = -0.508 \pm 0.049$ B. The confidence interval [–0.459; –0.557] complies well with both the result reported in the work by Mytsyk et al. [19] ($\pi_{66} = -0.47$ B) and the value measured by means of the four-point bending method [17] ($\pi_{66} = -0.573 \pm 0.079$ B). This implies that the experimental technique for measuring POCs based upon diametrically compressed disks is reliable

and could be successfully used to study crystalline and amorphous (glass) optical materials. Finally, now we are in a position to explain the inaccurate value of the POC π_{66} obtained for the LN crystals in our earlier work [18]. Namely, the reason is an unjustified choice of the fitting region equal to a full diameter of disk, instead of $0.80R$ as it should be. This factor should be necessarily taken into account when processing the retardation data set corresponding to the 'loading' diameter.

4. Conclusion

In the present work we have confirmed reliability and high precision of the experimental technique [18] suggested earlier for determination of POCs. The technique is based on producing a predetermined 2D distribution of mechanical stresses in a transparent material disk compressed along its diameter. The technique has been verified on the example of the parameter $\pi_{66} = \pi_{11} - \pi_{12}$ measured for the lithium niobate crystals. We have shown that this POC can be calculated with high enough accuracy. The sources of experimental errors appearing in the frame of this technique have been thoroughly analyzed and eliminated. The mean value $\langle\pi_{66}\rangle = \langle\pi_{11} - \pi_{12}\rangle$ derived in this study is equal to –0.508±0.049 B and agrees well with the corresponding POC values measured with the other methods. The absolute experimental error for the π_{66} coefficient is equal to 0.049 B, whereas the relative error does not exceed 10%.

References

1. Weber Y-J, 1995. Determination of internal strain by optical measurements. Phys. Rev. B. **51**: 12209–12215.
2. Narasimhamurty T S, Photoelastic and electrooptic properties of crystals. New York and London: Plenum Press (1981).
3. Slezinger I I, Alievskaya A N and Mironov Yu V, 1985. Piezo-optic devices. Izmeritelnaya Tekhnika. **12**: 17–19.
4. Kemp James C, 1969. Piezo-optical birefringence modulators: new use for a long-known effect. J. Opt. Soc. Amer. **59**: 950–954.
5. Balakshii V I, Parygin V N and Chirkov L E, Physical fundamentals of acoustooptics. Moscow: Radio i Sviaz' (1985).
6. Xu J and Stroud R, Acousto-optic devices: principles, design, and applications. New York: Wiley (1992).
7. Shaskolskaya M P, Acoustic crystals. Moscow: Nauka (1982).
8. Weber M J, Handbook of optical materials. Boca Raton: CRC Press (2003).
9. Pockels F, Lehrbuch der Kristallooptik. Berlin: Teubner (1906).
10. Mytsyk B H, 2003. Methods for the studies of the piezo-optical effect in crystals and the analysis of experimental data. Part I. Methodology for the studies of piezo-optical effect. Ukr. J. Phys. Opt. **4**: 1–26.
11. Vasylkiv Yu, Kvasnyuk O, Krupych O, Mys O, Maksymuk O and Vlokh R, 2009. Reconstruction of 3D stress fields basing on piezo-optic experiment. Ukr. J. Phys. Opt. **10**: 22–37.
12. Skab I, Smaga I, Savaryn V, Vasylkiv Yu and Vlokh R, 2011. Torsion method for measuring piezo-optic coefficients. Cryst. Res. Technol. **46**: 23–36.
13. Skab I, 2012. Optical anisotropy induced by torsion stresses in the crystals belonging to point symmetry groups 3 and $\bar{3}$. Ukr. J. Phys. Opt. **13:** 158–164.

14. Vasylkiv Yu, Savaryn V, Smaga I, Skab I and Vlokh R, 2011. On determination of sign of the piezo-optic coefficients using torsion method. Appl. Opt. **50**: 2512–2518.
15. Krupych O, Savaryn V, Skab I and Vlokh R, 2011. Interferometric measurements of piezo-optic coefficients by means of four-point bending method. Ukr. J. Phys. Opt. **12**: 150–159.
16. Krupych O, Savaryn V, Krupych A, Klymiv I and Vlokh R, 2013. Determination of piezo-optic coefficients of crystals by means of four-point bending. Appl. Opt. **52**: 4054–4061.
17. Krupych O, Savaryn V and Vlokh R, 2014. Precise determination of full matrix of piezo-optic coefficients with a four-point bending technique: the example of lithium niobate crystals. Appl. Opt. **53** (to be publish). http://dx.doi.org/10.1364/AO.53.0000B1
18. Vasylkiv Yu, Savaryn V, Smaga I, Krupych O, Skab I and Vlokh R, 2011. Studies of piezooptic coefficients in $LiNbO_3$ crystals using a crystalline disk compressed along its diameter. Ukr. J. Phys. Opt. **12**: 180–190.
19. Mytsyk B G, Andrushchak A S, Demyanyshyn N M, Kost' Y P, Kityk A V, Mandracci P and Schranz W, 2009. Piezo-optic coefficients of MgO-doped $LiNbO_3$ crystals. Appl. Opt. **48**: 1904–1911.
20. Frocht M M, Photoelasticity. London: J. Wiley and Sons (1965).
21. Vlokh R, Krupych O, Kostyrko M, Netolya V and Trach I, 2001. Gradient thermooptical effect in $LiNbO_3$ crystals. Ukr. J. Phys. Opt. **2**: 154–158.

Savaryn V, Krupych O and Vlokh R, 2014. Refined measurements of piezooptic coefficient π_{66} for the lithium niobate crystals, using a crystalline disk compressed along its diameter. Ukr. J. Phys. Opt. **15**: 30–37.

Анотація. *У роботі підтверджено високу точність і надійність запропонованого раніше експериментального методу вимірювання п'єзооптичних коефіцієнтів, який базується на заздалегідь відомому 2D розподілі механічних напружень у прозорому кристалічному або скляному диску, стиснутому вздовж діаметра. У роботі ретельно проаналізовано та усунуто джерела похибок експерименту. Отримане значення п'єзооптичного коефіцієнта π_{66} для кристалів ніобату літію добре узгоджується з літературними даними, визначеними за іншими методами.*